16th Australasian Wind Engineering Society Workshop
Brisbane, Australia
18-19 July, 2013

Development of Vulnerability Curves to Severe Wind Hazard of RC Low-rise Buildings with Roof Nail and Screw Fasteners

J.Y. Hernandez Jr., M.C.L. Veron, and B.M. Pacheco

Institute of Civil Engineering
University of the Philippines, Diliman, Quezon City 1101, Philippines

Abstract

Each year, an average of twenty (20) wind storms enter the Philippine Area of Responsibility causing slight to complete damage to low-rise residential buildings. In order to estimate the risk to severe wind hazard, the vulnerability of these types of buildings need to be quantified. In this paper, a computational procedure for developing fragility and vulnerability curves of RC low-rise residential buildings to severe wind hazard using computational fluid dynamics (CFD) is presented. Fragility curves for different damage states are derived considering variations in building attributes that strongly affect the pressure distributions generated during wind storms. This was performed for roof connected using nails and screws. Finally, the computational vulnerability curve is compared with observed data from the field.

Introduction

Among the different natural hazards that cause national disasters in the Philippines wind storms rank the highest in terms of disaster count, number of people killed or injured, number of people rendered homeless, total number of people affected, and total cost of damage. The average number of wind storms that enter the Philippine Area of Responsibility (PAR) is twenty (20), eight (8) of these make landfall causing disasters on their path. From 1901-2000, the Asian Disaster Reduction Center estimates the total cost of damage to be approximately 7,000 (in million US$) due to wind storms in the country. Comparing with earthquakes (rank #2 in terms of damage cost), the amount of damage is only 517 (in million US$) approximately (Aquino 2005).

There are different approaches to deriving vulnerability curves: analytical, empirical and heuristic method. In the analytical method, a computational fluid dynamics (CFD) approach is preferred because damage to non-structural elements such as the roof panels, windows, doors and walls are of interest. Thus, unlike most structural analysis methods that model the beams and columns as line elements, special finite elements and algorithms need to be used to capture fluid flow and the resulting pressure distributions on plane panels of a model structure. These can be effectively modelled using CFD. In this paper, the CFD module of the ANSYS general purpose finite element program, CFX, will be used in the modelling and analysis of wind flow on building structures.

Before a database of typical models are generated to capture damages that may occur on existing building structures, a sensitivity analysis will have to be conducted in order to identify those attributes of the buildings that greatly affect the pressure distribution and magnitudes due to severe wind. In a related research by the same authors, three attributes of residential buildings in Metro Manila are investigated: roof slope, roof eaves, and firewalls. The resulting wind pressure distributions are compared with those of a basis regular building model, observations are made and the effects of the different attributes are noted. The results show that changes in the roof slope greatly affect the pressure distribution, increasing the uplift forces (suction) with increased slope. The presence of firewalls that protrude on one side of the building generates high uplift forces on the corner between the firewall and the roof when the wind direction is perpendicular to the firewall. Lastly, the presence of roof eaves causes minor pressure magnitude changes but creates discernable changes to the wind pressure distribution observed in the model.

This paper discusses the development of an analytical vulnerability curve of reinforced concrete (RC) low-rise residential buildings to severe wind hazard, comparing vulnerability curves for structures that use roof nail and screw fasteners. The procedure initially derives fragility curves for different damage states and then the vulnerability curve is determined by summing the product of the damage index with the probability of exceedance of each damage state at different wind speeds. The vulnerability curve is validated using observed damage after typhoons with corresponding wind speed computed from typhoon simulations.

Methodology

During typhoons, it is frequently observed that the building envelope which includes the walls, doors, windows, and the roof are susceptible to damage by the resulting wind pressure and by wind-driven debris. It is then crucial to first identify building attributes which affect the magnitude and direction of wind pressure due to strong winds.

In a related study conducted by the authors (Hernandez and Veron 2012), different building models were generated for simulation and sensitivity analysis. First, the simplest gable-roofed structure is defined as the regular building. It has an approximately 26^0 roof slope (1:2), 3 m high ceiling, and plan dimensions of 6 x 10 m. Different building models are then created considering different building attributes that may affect the wind pressure distribution on the building due to severe wind loading. Building attributes that are normally found in houses found in Metro Manila were considered, namely: different roof slopes (1:3 and 1:1), presence of firewalls, presence of roof eaves, and presence of roof eaves and fire walls together.

The results of the initial study show that different non-structural attributes (roof slope, roof eaves, and firewalls) affect the wind velocity streamline patterns generated, causing changes in the wind pressure distribution on roofs and walls of buildings. Changes in roof slope affect the resulting wind pressure, not only in terms of its magnitude and distribution, but also its direction (suction or compression) on the same roof area. The presence of firewalls generates high suction wind pressure on the roof at the corner area of the firewall and the roof. This is attributed to the induced pressure gradient as the flow separates from the boundary layer at the firewall and then reattaches to the roof at a

distance from the firewall. The presence of roof eaves affects the wind pressure distribution on the windward side of the building, causing the flow to separate from the roof at the eaves. The change in magnitude of the pressures is minor but there is a discernable change in the wind pressure distribution. Thus it is very important to include in the models these non-structural attributes, aside from floor area, roof material, and window material, when deriving vulnerability curves for residential buildings considering severe wind loading.

In the methodology used, shown in Figure 1, the fragility curves for slight, moderate, extensive, and complete damage states are first derived for a population of building models that incorporate different building attributes which affect the behaviour of the structure when subjected to wind loading. Building attributes that are considered in the building database include differing roof angles, floor area, one- and two-storey buildings, roof material, window material, roof eaves and fire walls. Definitions of different damage states from Hazus-MH (Vickery et al. 2006) are followed. Moreover, three different wind directions were considered in the analysis: longitudinal, lateral, and inclined at a 450 angle. The wind pressure distribution on a model building is determined per wind speed using computational fluid dynamics (CFD) in ANSYS CFX. The effect of turbulence is also included in the analysis. Figure 2 shows a sample model of a residential building with resulting wind pressure distribution. The damage state is determined by comparing the wind pressure on the building surface to threshold values determined from experimentation. After completing the analysis of all models, the percent (%) probability of exceedance of a damage state is computed for each wind speed used, providing data points for the fragility curves. Then cumulative probability distribution functions are fitted to the data points for slight, moderate, extensive and complete damage. The resulting curves are the fragility curves of the building. With the fragility curves, the final step involves the use of a corresponding damage index per damage state to derive the vulnerability curve. Figure 3 shows the vulnerability curve of the structure.

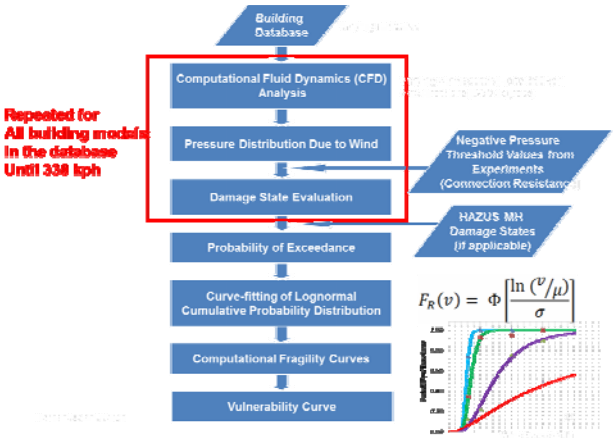

Figure 1. Computational Method used for Developing Vulnerability Curves to Severe Wind Hazard

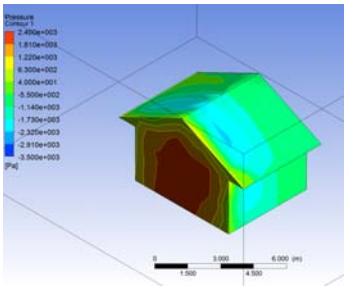

Figure 2. Sample Model Wind Pressure Distribution

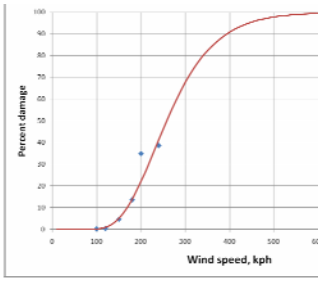

Figure 3. Sample Vulnerability Curve

Threshold Values

The capacity of each building envelope against strong winds depends on its material and connections. Roofs may be fastened using nails on wood or using screws on steel purlins. Windows may be made of wood or glass, while walls may be made of wood, steel or masonry. It is therefore critical to determine the threshold value of each building envelope and its materials. Threshold values of the building envelope are compared to the resulting wind pressure. Damage occurs when wind pressure exceeds the uplift threshold values. This paper adopts the threshold values resulting from experimentations as shown in Table 1. The 1200 Pa is the uplift capacity of the roof sheathing using 6d nails (Lee and Rosowsky 2005) while the 4300 Pa is the wind rating of the roof system using screws(Baskaran et al 2009).

Material	Threshold Values (Pa)	Reference
Roof Nail	1200	Lee and Rosowsky, 2005
Roof Screw	4300	Baskaran, Ko and Molleti, 2009
Glass Window	3332	Cope 2004

Table 1. Threshold Values used in the analysis for different roof fasteners and for glass window.

Once areas in the building envelope exceed the threshold values, the model is revised to simulate damage by introducing holes on the building envelope.

Damage States

The quantification of the damage state of a building due to strong winds is adopted from definitions of Hazus-MH (Vickery et al. 2006). This is shown in Table 2. For minimal damage on the roof cover and no damage on walls and windows, the building is considered to have no damage to very minor damage. For a slightly damaged roof cover and a maximum of one window damaged, the building is considered to be slightly damaged. For a moderately damaged roof cover and a maximum of three windows damaged, the building is considered to be moderately damaged A severely damaged building has major roof damage and most of the windows are broken. Complete damage is when the frame of the building already failed. Damaged states are developed depending on the percent loss of each of the building envelope shown in Table 2.

Discussion of Results

Damage states of residential buildings for each wind speed and direction were recorded as shown in Table 3. The probability of occurrence and the percent exceedance of each damage state were calculated as listed in Tables 4-6. In Table 4, the frequency of occurrence is determined by summing the number of models that experience a specific damage state of a particular wind speed. Then the percent (%) probability of occurrence is determined by dividing the frequency of occurrence by the total number of models, this is shown in Table 5. Finally, the percent probability of exceedance is computed by taking the cumulative percent probabilities under each of the damage states.

Damage State	Qualitative Damage	Roof Cover Failure	Window/ Door Failure	Roof Structure Failure	Wall Structure Failure
0	No damage or very slight damage	≤ 2%	None	No	No
1	Slight damage	2% < x ≤ 15%	1	No	No
2	Moderate damage	15% < x ≤ 50%	1 < x < (20% or 3)	No	No
3	Extensive Damage	>50%	(20% or 3) < x ≤ 50%	No	No
4	Complete Damage	>50%	>50%	Yes	Yes

Table 2. Hazus-MH damage states for Wind Vulnerability Curves.

Model	Wind Direction	Wind Speed (kph)				
		180	250	270	300	350
1	longitudinal	S	M	E	C	C
	lateral	S	S	M	M	E
	45 deg	S	E	E	E	C
2	longitudinal	S	M	E	E	E
	lateral	S	S	M	E	E
	45 deg	S	M	M	E	E
3	longitudinal	S	E	E	C	C
	lateral	S	S	E	C	C
	45 deg	S	M	M	E	E
4	longitudinal	S	E	E	C	C
	lateral	ND	M	E	C	C
	45 deg	S	E	C	C	C
5	longitudinal	S	S	E	E	E
	lateral	M	E	C	C	C
	45 deg	M	E	C	C	C
6	longitudinal	S	S	M	M	M
	lateral	M	E	C	C	C
	45 deg	M	E	C	C	C
7	longitudinal	S	E	E	E	C
	lateral	S	E	C	C	C
	45 deg	M	E	E	E	C
8	longitudinal	M	E	C	C	C
	lateral	S	E	C	C	C
	45 deg	S	E	E	E	C
9	longitudinal	S	E	C	C	C
	lateral	S	M	E	C	C
	45 deg	S	E	E	E	C
10	longitudinal	S	M	M	M	M
	lateral	S	E	C	C	C
	45 deg	S	E	C	C	C
11	longitudinal	S	E	E	C	C
	lateral	S	M	E	E	C
	45 deg	S	E	E	E	C

Table 3. Record of state damages of RC low-rise building with roof nails

Damage State	180 kph	250 kph	270 kph	300 kph	350 kph
No Damage	1	0	0	0	0
Slight	26	5	0	0	0
Moderate	6	8	6	3	2
Extensive	0	20	16	12	6
Complete	0	0	11	18	25

Table 4 Frequency of damages for each wind speed for RC low-rise building with roof nails

Damage State	180 kph	250 kph	270 kph	300 kph	350 kph
No Damage	3.0	0	0	0	0
Slight	78.8	15.2	0	0	0
Moderate	18.0	24.0	18.2	9.1	6.1
Extensive	0	61.0	48.0	36.4	18.2
Complete	0	0	33.0	55.0	76.0

Table 5 Probability of occurrence of damages for each wind speed for RC low-rise building with roof nails

Damage State	180 kph	250 kph	270 kph	300 kph	350 kph
No Damage	100.0	100.0	100.0	100.0	100.0
Slight	97.0	100.0	100.0	100.0	100.0
Moderate	18.0	85.0	100.0	100.0	100.0
Extensive	0	61.0	82.0	90.9	93.9
Complete	0	0	33.0	55.0	76.0

Table 6 Percent probability of exceedance of damages for each wind speed for RC low-rise building with roof nails

A similar procedure was used considering roof screws as the fasteners. Then, fragility curves were fitted using the lognormal cumulative distribution function given by,

$$F(v) = \Phi\left[\frac{\ln(v/\mu)}{\sigma}\right] \quad (1)$$

Where v is wind speed, $\Phi[.]$ is the standardized normal distribution function, and the fragility parameters μ and σ are the mean and standard deviation. The resulting fragility curves of RC Low-rise residential buildings are shown in Figures 4 and 5.

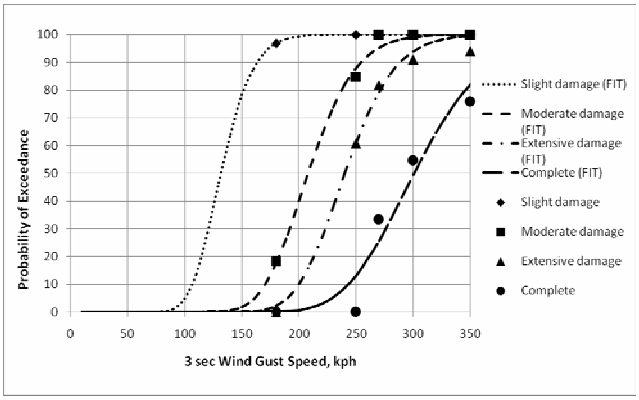

Figure 4 Fragility curves for RC low-rise buildings using roof nail

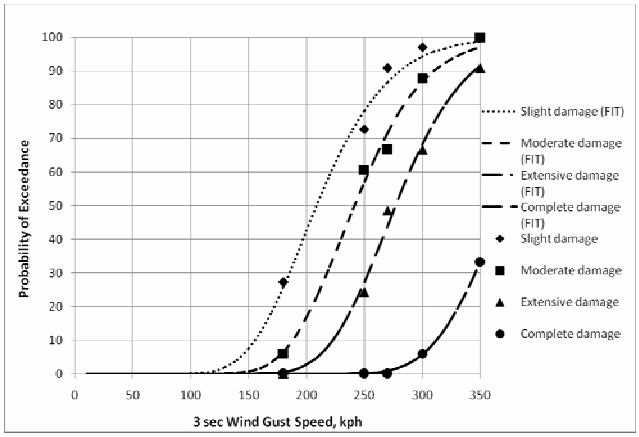

Figure 5 Fragility curves for RC low-rise buildings using roof screw

With the fragility curves, the final step involves the use of a corresponding damage index per damage state to derive the vulnerability curve. The damage indices were determined by approximating the percent cost of repairing the building for each damage state. For example, the estimated percent cost of the roof and the windows of a residential building are 30% and 10%

respectively. However, for moderate damage, only 15% to 50% of the roof is damaged and 20% of the windows damaged. Calculating the percent cost of repairing a moderately damaged building would then be 4.5 to 17%. Its median is the damage index for moderate damage. The computed damage indices are shown in Table 7.

Damage State	Damage Indices
None	0.00
Minor	0.01
Moderate	0.10
Extensive	0.19
Complete	0.40

Table 7 Damage Indices

Damage indices were used as multipliers to probability of occurrences of state damages to determine the data points of the vulnerability curves. The points are then fitted using the lognormal cumulative distribution function given by,

$$V(v) = \Phi\left[\frac{\ln(v/\mu)}{\sigma}\right] \quad (2)$$

Where v is wind speed, $\Phi[.]$ is the standardized normal distribution function, and the vulnerability parameters μ and σ are the mean and standard deviation.

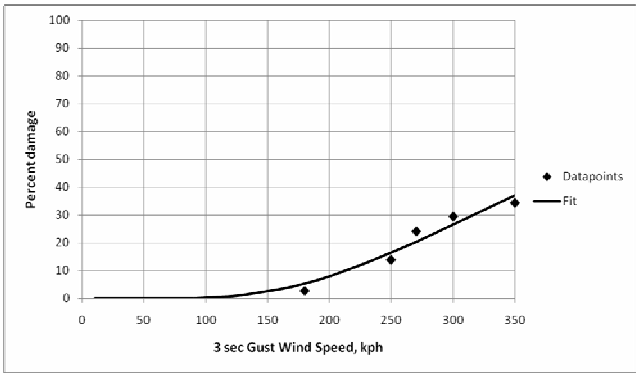

Figure 6 Vulnerability curve for RC low-rise buildings using roof nail

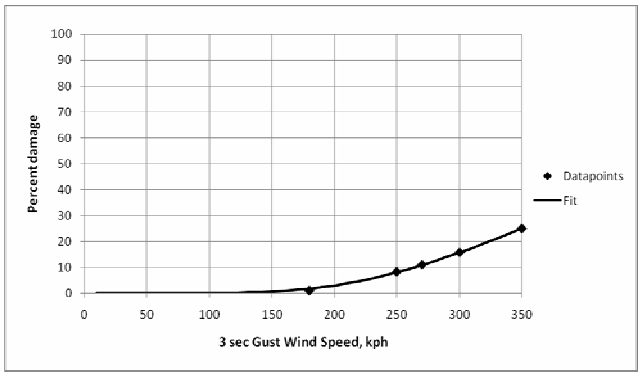

Figure 7 Vulnerability curve for RC low-rise buildings using roof screw

Most of the damage observed in reinforced concrete (RC) low-rise residential buildings are damages on the roof cover. As the roof is 30-40% of the total cost of the building, most of the damage data points are below 40%. It is unlikely to see the RC frame damaged. As a means of validating the derived vulnerability curve, observed damage of residential buildings provided by the Philippine Atmospheric Geophysical Astronomical Services Administration (PAGASA) were plotted with the vulnerability curve shown in Figure 8. It can be observed that the vulnerability curve estimates well at what speed damage starts. However, there are data points from observed damage that plot quite far from the curve. It is possible that these are outliers because the standards for engineered construction may not have been followed for buildings in the provinces.

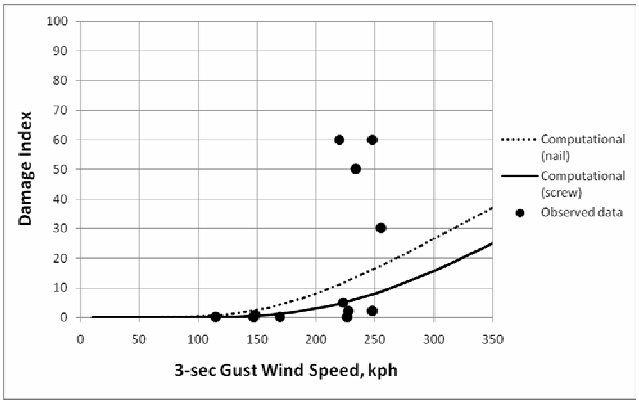

Figure 8 Comparison of Computational Vulnerability Curves of Buildings with Nail and Screw Fasteners to Observed Field Data

Conclusions

The vulnerability curves of RC low-rise buildings with roof nails and screw fasteners were developed using CFD. The threshold values for uplift wind pressure were used to determine the different damage states experienced by model structures. With the frequency of occurrence of a damage state computed for different wind speeds, the fragility curves for slight, moderate, extensive, and complete damage states can be plotted. Then the vulnerability curves are determined using damage indices for each damage state.

Acknowledgments

The authors would like to thank the Philippine Atmospheric Geophysical Astronomical Services Administration (PAGASA), the Philippine Institute for Volcanology and Seismology (PHIVOLCS), Geoscience Australia (GA), and AusAID for their financial and technical support of this project.

References

Anderson, J.Jr.D. (1995) Computational Fluid Dynamics: The Basics with Applications. McGraw-Hill, Inc.

ANSYS CFX Software v.13.

Aquino, R.E.R. (2005) Philippine Wind Information for Engineering, Research, and Mitigation. Report for COE Short-term Fellowship Program, 13 June 2005.

Baskaran, B.A., Ko, S.K.P., Molleti, S. (2009) A novel approach to estimate the wind uplift resistance of roofing systems, Building and Environment, Vol. 44, Elsevier B.V., pp. 723-735.

Holmes, J.D. (2001) Wind Loading of Structures. SPON Press, Taylor and Francis Group.

Lee, K.H., Rosowsky, D.V. (2005) Fragility assessment for roof sheathing failure in high wind regions, Engineering Structures, Vol. 27, Elsevier B.V., pp. 857-868.

Vickery, P.J., Skerlj, P.F., Lin, J., Twisdale, L.A. Jr., Young, M.A., Lavelle, F.M. (2006) HAZUS-MH Model Methodology II: Damage and Loss Estimation, ASCE National Hazards Review, Vol.7, No.2, pp. 94-103.